PCCP

ROYAL SOCIETY OF CHEMISTRY

PAPER

View Article Online
View Journal | View Issue

Cite this: *Phys. Chem. Chem. Phys.*, 2021, **23**, 17265

Reversible photoluminescence modulation of monolayer MoS_2 on a ferroelectric substrate by light irradiation and thermal annealing†

Peng Wang,[ab] Jian Wang,[a] Yun Zheng,[a] Hongyan Shi,[ac] Xiudong Sun,[ac] Wenjun Liu[b] and Bo Gao *[ac]

Received 21st May 2021,
Accepted 14th July 2021

DOI: 10.1039/d1cp02248b

rsc.li/pccp

Monolayer semiconducting two-dimensional (2D) materials are strongly emerging materials for exploring the spin-valley coupling effect and fabricating novel optoelectronic devices due to their unique structural symmetry and band structures. Due to their atomic thickness, their excitonic optical response is highly sensitive to the dielectric environment. In this work, we present a novel approach to reversibly modulate the optical properties of monolayer molybdenum disulfide (MoS_2) *via* changing the dielectric properties of the substrate by laser irradiation and thermal annealing. We chose $LiNbO_3$ as the substrate and recorded the PL spectra of monolayer MoS_2 on $LiNbO_3$ substrates with positive (P^+) and negative (P^-) ferroelectric polarities. A distinct PL intensity of the A peak was observed due to opposite doping by surface charges. Under light irradiation, the PL intensity of monolayer MoS_2 on P^+ Fe_2O_3-doped $LiNbO_3$ gradually decreased with time due to the reduction of intrinsic p-doping, which originated from the drift of photo-excited electrons under a spontaneous polarization field and accumulation on the surface. The PL intensity was found to be restored by thermal annealing which could erase the charge redistribution. This study provides a strategy to reversibly modulate the optical properties of monolayer 2D materials on top of ferroelectric materials.

1. Introduction

Two-dimensional (2D) materials have attracted intense research interest both in theory and experiment due to their fascinating crystal lattice structures and electronic properties in the past few decades. Layered transition metal dichalcogenides (TMDs), which are semiconductors with a chemical formula MX_2 (M = Mo, W, *etc.*; X = S, Se, Te), have been extensively investigated owing to their unique electrical and optical properties.[1–7] In particular, monolayer TMDs, whose band structure evolves from indirect gap to direct gap, produce a strong exciton pumping efficiency with energy gaps located at the Brillouin zone owing to the atomically thin structure.[8–11] Monolayer TMDs provide a platform for investigating tightly bound excitonic states, spin-valley coupling, optically controlled valley polarization and coherence,[12–17] and hence are regarded as a promising class of materials for next-generation state-of-art micro/nano optoelectronic devices. It is usually essential to modify and modulate the electronic, chemical and optical properties of 2D materials for a wide range of applications in flexible electronics,[18–20] gas sensors,[21] transistors[10] and biosensors.[22] So far, many strategies have been developed to modulate the optical properties of 2D materials, including chemical doping, electrostatic gating and structuring. In the case of electrostatic gating, a field-effect transistor (FET) configuration was usually employed to reversibly regulate the number of charge carriers in 2D materials.[23–26] However, the metal gates require additional processing steps and result in inhomogeneous spatial distribution of charge carriers,[27,28] and the metallic contact with TMDs could quench the light emission at the interface. To overcome these disadvantages, many other novel methods have been put forward to modulate the charge transport and optical properties of 2D TMDs, such as light irradiation, substrate induction, or environment assistance.

Due to the pronounced photorefractive, pyroelectric and piezoelectric properties, lithium niobate ($LiNbO_3$) has been

[a] *Institute of Modern Optics, School of Physics, Key Laboratory of Micro-Nano Optoelectronic Information System, Ministry of Industry and Information Technology, Key Laboratory of Micro-Optics and Photonic Technology of Heilongjiang Province, Harbin Institute of Technology, Harbin 150001, China. E-mail: gaobo@hit.edu.cn*

[b] *Department of Physics, Harbin Institute of Technology at Weihai, Weihai 264209, China*

[c] *Collaborative Innovation Center of Extreme Optics, Shanxi University, Taiyuan 030006, China*

† Electronic supplementary information (ESI) available: Evaluation of the PDMS transfer process and PL spectra of as-grown MoS_2 before transfer. See DOI: 10.1039/d1cp02248b

used in electro-optical modulators, surface acoustic wave devices, piezoelectric sensors and holographic recording.[29–31] It is unfortunate that $LiNbO_3$ is a wide-gap insulator which limits its application in optoelectronics. Recently, the concept of integrating $LiNbO_3$ and semiconductor materials has been proposed.[30,31] By transferring monolayer $MoSe_2$ and WSe_2 onto the surface of domain-engineered $LiNbO_3$, their photoluminescence (PL) was significantly enhanced or inhibited,[32] because reversible and nonvolatile control of TMD doping was induced by opposite surface charges on the $LiNbO_3$ substrate with different domain orientations. It is known that local light irradiation could redistribute the space charge in $LiNbO_3$ due to the migration and stable trapping of photo-excited electrons,[33] which could change its dielectric properties and may affect the charge transport and optical properties of 2D TMDs on top. It is also reported that the trapped electrons could be re-activated and the charge distribution could be restored by thermal annealing[34–37] or uniform UV light irradiation,[38] which might have an opposite effect on 2D TMDs to light irradiation. Therefore, it is possible to reversibly modulate the optical properties of 2D TMDs on $LiNbO_3$ by combining light irradiation and thermal annealing, which are nondestructive and noncontact techniques.

In this work, we present a novel approach to reversibly modulate the optical properties of monolayer MoS_2 *via* changing the dielectric properties of the substrate by laser irradiation and thermal annealing. Our approach is based on $LiNbO_3$, a widely known ferroelectric material for various optical and acoustic applications. Due to the inherent surface charges, the polarized $LiNbO_3$ was found to change the doping and hence the PL of the supported monolayer MoS_2. After that, using laser we irradiated Fe_2O_3-doped $LiNbO_3$ with a positive ferroelectric polarity to excite and accumulate electrons on the surface under a spontaneous polarization field, and found that the PL intensity of the A peak of the supporting monolayer MoS_2 decreased with irradiation time. After thermally annealing the irradiated sample to erase the charge redistribution, the PL intensity of the A peak was restored. This study demonstrated a reversible PL modulation of monolayer 2D materials by optically irradiating and thermally annealing the beneath ferroelectric substrates.

2. Experimental

2.1 CVD growth of monolayer MoS_2 on SiO_2/Si

Monolayer MoS_2 was grown on SiO_2/Si substrates with 300 nm of SiO_2 by chemical vapor deposition (CVD). Briefly, solid state precursors of MoO_3 and sulfur powder were loaded into a 1-inch quartz tube with a distance of 18 cm. A firebrick crucible filled with sulfur powder was placed upstream in the quartz tube outside the furnace, and an alumina crucible filled with MoO_3 powder was loaded in the center of the furnace. The sulfur vapor was introduced by Ar to react with molybdenum oxide (MoO_x from MoO_3) at an elevated temperature (660 °C) for monolayer MoS_2 growth by sulfurization reactions. In order to acquire large-size monolayer MoS_2 with high quality, we used traces of alkali metal compounds as promoters to facilitate the growth. Monolayer WS_2 was synthesized at 850 °C by using solid WO_3 and S precursors.

2.2 Transfer of monolayer MoS_2 onto a ferroelectric substrate

To avoid possible contamination, freshly made PDMS was used for transferring monolayer MoS_2 from SiO_2/Si onto a $LiNbO_3$ substrate, as schematically shown in Fig. 1a. A piece of PDMS was attached onto the MoS_2-covered SiO_2/Si surface and was immersed into deionized (DI) water. Then, the PDMS, adhering MoS_2, was gently peeled from the SiO_2/Si surface. Subsequently, the

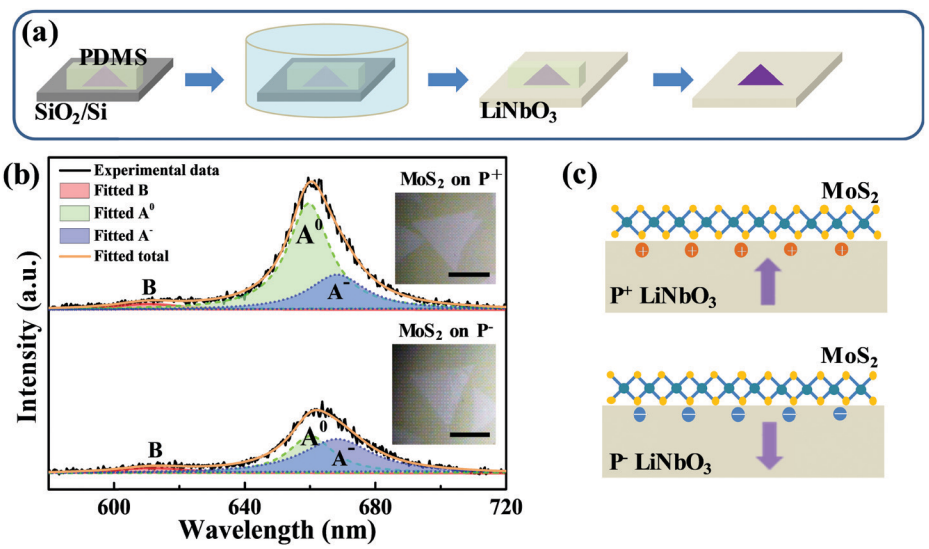

Fig. 1 (a) Schematic illustration of the PDMS-assisted transfer process developed in this work. (b) Micro-PL spectra of monolayer MoS_2 on $LiNbO_3$ with positive ferroelectric polarity (P^+) and negative polarity (P^-). The dotted lines show the fitted peaks. Insets show the corresponding optical images of the monolayer MoS_2. Scale bars: 25 μm. (c) Schematic illustration of the induced surface charges and the expected doping effect on monolayer MoS_2. Purple arrows depict the polarized orientation of the $LiNbO_3$ substrate.

MoS_2-covered PDMS was taken out of DI water and attached onto the $LiNbO_3$ surface. After baking in a vacuum oven at 60 °C for 5 min, the PDMS was peeled from the $LiNbO_3$ surface, leaving MoS_2 on the $LiNbO_3$ substrate. To eliminate the possible variance of different batches of CVD-grown MoS_2 on SiO_2/Si, the as-grown sample was sliced into several parts and separately transferred onto different substrates. The control experiment involving the transfer onto the hydrophilic SiO_2/Si substrate shows that the morphology and optical properties of MoS_2 could be well preserved (Fig. S1, ESI†).

2.3 Characterization

A continuous wave 532 nm laser with a power of 40 μW and a spot size of ~1 μm was used for long-time illumination to form charge redistribution. Thermal annealing was carried out in a heating/cooling stage (HCS321Gi, INSTEC Inc.) to restore the $LiNbO_3$ substrate to uniform charge distribution. Micro-Raman and -PL spectra were collected to characterize the optical properties of monolayer MoS_2 and WS_2 on various substrates (NT-MDT NTEGRA Spectra). The morphology of monolayer MoS_2 and WS_2 on $LiNbO_3$ was characterized by optical microscopy (OLYMPUS BX51).

3. Results and discussion

The as-grown monolayer MoS_2 has uniform light emission (Fig. S2, ESI†), providing an excellent prototype for this study. Fig. 1b shows the typical PL spectra of monolayer MoS_2 on *z*-cut $LiNbO_3$ substrates with positive (P^+) and negative (P^-) ferroelectric polarities, which were recorded under a pump power of 40 μW to avoid any heating and oxidation effects. The insets show the optical images. Both samples exhibit a clean surface and well-known A and B peaks, confirming the high quality of transferred monolayer MoS_2. But the PL intensity of the A peak from monolayer MoS_2 on the P^+ $LiNbO_3$ substrate was enhanced, while on the P^- $LiNbO_3$ substrate the PL intensity of the A peak was suppressed. The PL intensity of the B peak had no differences between the two samples. To clearly show the spectral differences, the A peak in the PL spectra was fitted by two Lorentzian peaks corresponding to neural exciton (A^0) and trion exciton (A^-), respectively (Fig. 1b). It can be seen that the PL intensity of A^0 on the P^+ substrate was much larger than that on the P^- substrate, while the PL intensity of A^- did not change, resulting in a larger PL intensity ratio between A^- and A on the P^- substrate. This, along with the distinct A peak intensity, indicates more p-type doping on the P^+ substrate and more n-type doping on the P^- substrate, which are due to the distinct dielectric environment of the $LiNbO_3$ surface originating from the polarized state.[32] Fig. 1c schematically shows the $LiNbO_3$-induced doping effect on monolayer MoS_2. The P^+ $LiNbO_3$ substrate has an up-polarized state, in which the positive surface charges accumulate and enhance the intrinsic p-type character of MoS_2.[39,40] In contrast, the P^- $LiNbO_3$ substrate has a down-polarized state, resulting in rich negative surface charges and hence n-type doping of monolayer MoS_2. The distinct p- and n-type doping would enhance and suppress the PL emission, respectively. Due to the unfortunate overlap of vibrational modes of MoS_2 and $LiNbO_3$, Raman spectroscopy, which is also an easy indicator for doping of monolayer MoS_2, could not be used in this work.

As a photorefractive material, light irradiation is believed to produce space charge distribution in $LiNbO_3$ due to the migration and stable trapping of photo-excited electrons, providing the possibility of modulating the optical properties of the supporting MoS_2. Fig. 2a and b show the PL spectra of monolayer MoS_2 on P^+

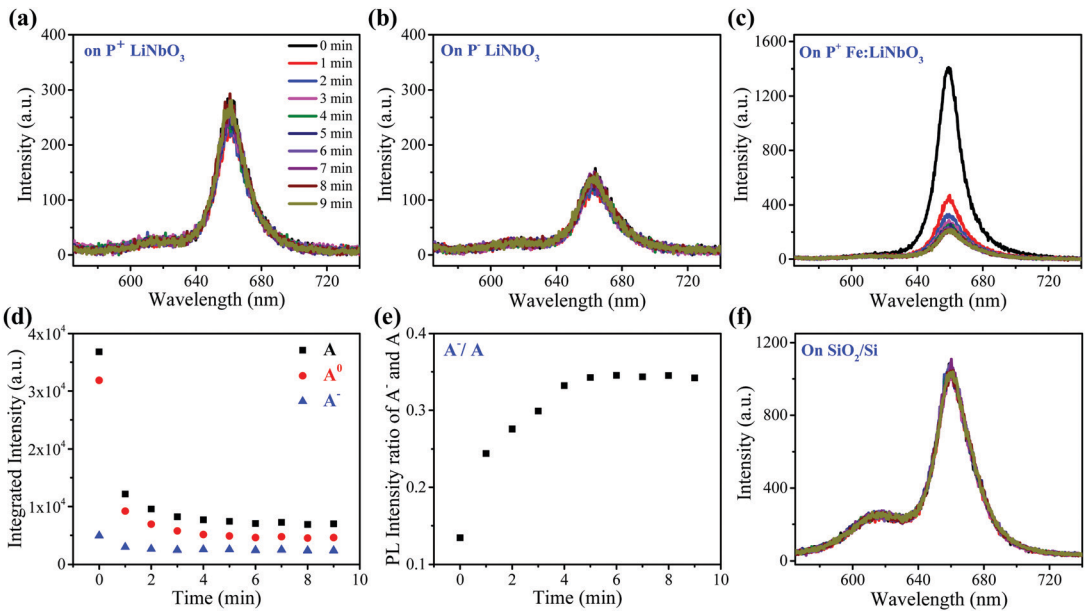

Fig. 2 PL spectra of monolayer MoS_2 on (a) P^+ $LiNbO_3$, (b) P^- $LiNbO_3$ and (c) P^+ Fe:$LiNbO_3$ for laser irradiation time up to 9 min, respectively. (d) Integrated PL intensity of A^0, A^- and A peaks and (e) PL intensity ratio of A^- and A from monolayer MoS_2 on P^+ Fe:$LiNbO_3$ as a function of laser irradiation time. (f) PL spectra of monolayer MoS_2 on SiO_2/Si for laser irradiation time up to 9 min.

and P^- $LiNbO_3$ substrates for laser irradiation time up to 9 min. It can be seen that the PL intensity remains nearly constant with the laser irradiation time for both P^+ and P^- $LiNbO_3$ substrates, which is possibly due to the low optical response of pure $LiNbO_3$.[34,41,42]

In order to enhance the optical response of $LiNbO_3$ for the modulation of the optical properties of MoS_2, we used z-cut Fe_2O_3-doped $LiNbO_3$ with a positive ferroelectric polarity (P^+ Fe:$LiNbO_3$) as the substrate. Fig. 2c shows the PL spectra of monolayer MoS_2 on the P^+ Fe:$LiNbO_3$ substrate for laser irradiation time up to 9 min. The PL intensity of monolayer MoS_2 was much larger than that on undoped $LiNbO_3$ due to the presence of Fe ions. After laser irradiation, the PL intensity of the B peak had no obvious changes, while the PL intensity of the A peak changed. To clearly show the variation tendency, the PL spectra were fitted. Fig. 2d shows the integrated intensity of A^0, A^- and A peaks as a function of laser irradiation time, all of which have similar tendency. In the first 1 min, the PL intensity of the A peak decreased sharply. Within subsequent 2–4 min, the PL intensity slightly decreased. After 4 min, the intensity remained almost constant. Besides, we plotted the intensity ratio of A^- and A peaks as a function of laser irradiation time, which was found to increase (Fig. 2e). The decrease of the intensity and the increase of the intensity ratio with irradiation time are similar to the change of the A peak when employing a gate voltage[43,44] and functionalizing MoS_2 with n-type molecules.[40,45] We also recorded the PL spectra of monolayer MoS_2 on the SiO_2/Si substrate as a function of irradiation time as a control experiment. It can be seen that the PL intensity remained nearly constant as the irradiation time increased, indicating that the Fe:$LiNbO_3$ substrate played a vital role in the PL change.

The PL change of monolayer MoS_2 on P^+ Fe:$LiNbO_3$ as a function of laser irradiation time was attributed to the modulation of the surrounding dielectric environment, as schematically shown in Fig. 3. The doped Fe ions in Fe:$LiNbO_3$ have two valence states, Fe^{2+} and Fe^{3+}, which act as photo-excited charge centers to produce electrons or holes under light irradiation, and govern the migration of free photo-excited electrons according to the following scheme:[34]

$$Fe^{2+} + h\nu \rightarrow Fe^{3+} + e \quad (1)$$

Due to the lower valence state, Fe^{2+} impurity sites can act as donors to supply electrons to the conduction band. The photo-excited electrons migrate freely in the lattice. Two main effects dominate the migration: the spontaneous polarization field and concentration gradient of free electrons. The former originates from the asymmetry of the crystalline structure of $LiNbO_3$, which results in a spontaneous polar moment. The orientation of the polar moment of each cell in a polarized ferroelectric crystal is consistent, which is equivalent to an internal electric field. As shown by the solid arrows in Fig. 3b, the photo-generated electrons drift under the action of the electric field, which is also named photovoltaic effect. The latter originates from the concentration gradient of free electrons between the irradiation area and the dark region in the $LiNbO_3$ crystal.[46] As shown by the dotted arrows in Fig. 3b, photo-excited electrons diffuse away from the irradiation area to the dark region, and get trapped by acceptor sites of Fe^{3+}. The scheme of this capture process can be interpreted as follows:

$$Fe^{3+} + e \rightarrow Fe^{2+} \quad (2)$$

The drift of the excited electrons redefines the local dielectric environment at the surface of $LiNbO_3$.

Most notably, the areal charge density of the positive *z*-cut face of $LiNbO_3$ can reach as large as $\sigma^z = 0.7$ C m^{-2} due to its spontaneous polarization, producing a large internal electric field. Excited electrons prefer to be controlled by the electric field rather than diffusing away. When the electrons arrive at the positive surface of P^+ Fe:$LiNbO_3$, the initial doping effect of MoS_2 by polarized surface charge will be reduced, resulting in the modulation of PL emission. However, the concentration of the dopant limits the number of excited electrons in $LiNbO_3$. As the irradiation time increased, the concentration of photo-excited electrons gradually decreased until it reached the limit.[47,48] Under the experimental conditions in this work, the drift of photo-excited electrons to the surface was mainly achieved in the first 1 min, decreasing the PL intensity of MoS_2 sharply. In the subsequent 2–4 min, the doping effect gradually became insensitive to laser illumination time as the concentration of photo-excited electrons decreased. After 4 min, the PL intensity of MoS_2 remained almost constant due to the complete depletion of Fe^{2+} ions which is responsible for the redistribution of the surface charge. In pure $LiNbO_3$, due to the low density of excited electrons, few charge carriers were optically excited and no PL modulation could be observed.

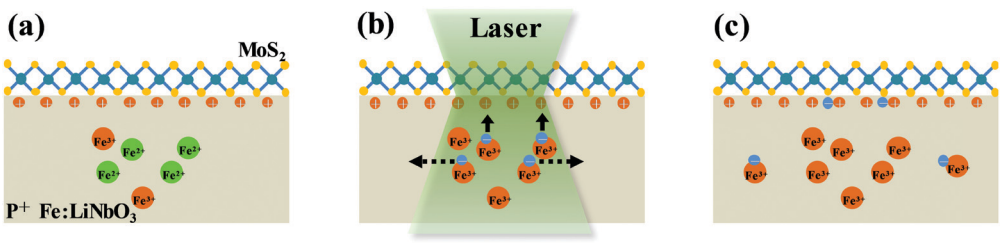

Fig. 3 Schematic illustration of the dielectric environment of monolayer MoS_2 on P^+ Fe:$LiNbO_3$ under laser irradiation. (a) Positive ferroelectric polarity and its induced surface charge. (b) Drift and diffusion of the excited electrons. The solid arrows depict the drift effect of photo-excited electrons under a spontaneous polarization field, while the dotted arrows depict the diffusion due to the concentration gradient. (c) The electrons arriving at the positive surface of P^+ Fe:$LiNbO_3$ reduce the initial doping effect of MoS_2 produced by polarized surface charges.

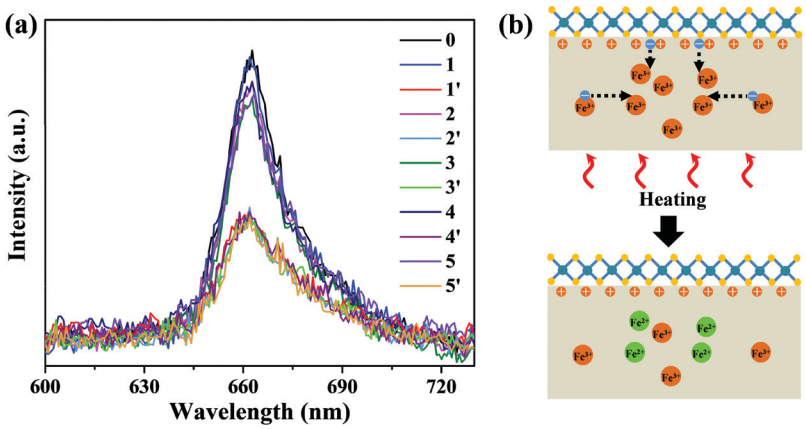

Fig. 4 (a) Reversible modulation of PL intensity for 5 cycles by laser irradiation and thermal annealing. (0) PL spectra of monolayer MoS_2 on P^+ Fe:$LiNbO_3$ before laser irradiation. (1–5) PL spectra after laser irradiation and (1′–5′) restored PL spectra after thermal annealing. (b) Schematic illustration of erasing the charge redistribution in P^+ Fe:$LiNbO_3$ *via* thermal annealing.

It is known that the resulting charge redistribution, existing for a long period due to the deep trap state, could be erased by thermal annealing[34–37] or uniform UV light irradiation.[38] In order to avoid possible damage to MoS_2 by UV light,[49] we chose thermal annealing to erase the charge redistribution, which was performed in a heating/cooling stage at 150 °C for 20 min in argon to restore P^+ Fe:$LiNbO_3$ to the initial state. The heating/cooling stage was placed on a home-built confocal microscope for *in situ* PL measurement. Fig. 4a shows the PL spectra of monolayer MoS_2 on P^+ Fe:$LiNbO_3$ before laser irradiation (black curve), after laser irradiation (blue curve) and after thermal annealing (red curve). Similar to those in Fig. 3, the PL intensity decreased after laser irradiation for 9 min. But subsequent thermal annealing restored the PL intensity. Fig. 4b schematically illustrates the erasing of charge redistribution in P^+ Fe:$LiNbO_3$ *via* thermal annealing. The electrons on the surface are activated by heating, and then diffuse at high temperatures until captured by Fe^{3+}. In the meantime, the heating provides the activation energy to excite the electronic charge in Fe^{3+} traps, which diffused back to the light irradiation area.[35,48] The overall effect is the erasing of charge redistribution produced by light irradiation. Therein, the migration of the surface electrons and hence recovery of the surface charge states lead to the restoration of the PL intensity. In order to explore the reversibility over time, we performed laser illumination and thermal annealing for another four cycles. It can be seen that the reversible PL modulation could be well achieved after five cycles, suggesting long-time reversibility.

Besides, we carried out experiments using CVD-grown monolayer WS_2, and reversible PL modulation was also achieved for monolayer WS_2 on the P^+ Fe:$LiNbO_3$ substrate by light irradiation and thermal annealing (Fig. S3, ESI†), suggesting that the reversible modulation strategy could be universally extended to other 2D materials.

4. Conclusions

In this work, we have successfully achieved PL modulation in monolayer MoS_2 by light irradiation and thermal annealing by using a ferroelectric $LiNbO_3$ substrate. The PL intensity of the A peak of monolayer MoS_2 was enhanced/suppressed due to the p-/n-doping by the positive/negative polarized charge on the P^+/P^- $LiNbO_3$ substrate. Under light irradiation, the PL intensity of the A peak of monolayer MoS_2 on the P^+ Fe:$LiNbO_3$ substrate gradually decreased with time, and was restored after thermal annealing. This change is due to the reduction and the recovery of intrinsic p-doping of monolayer MoS_2, which originated from the light-induced redistribution and heat-activated recovery of the surface charge. This study provides a strategy to reversibly modulate the optical properties of monolayer 2D materials on top of ferroelectric materials, which could have a great potential application in the fields of information encryption, data storage and memory chips.

Author contributions

B. G. initiated the idea. P. W. and H. S. did the experiment. All authors analyzed and interpreted the data. P. W. and B. G. wrote the manuscript. B. G. supervised the project.

Conflicts of interest

The authors declare no competing financial interest.

Acknowledgements

This work was financially supported by the National Natural Science Foundation of China. (No. 91956129 and 21973023).

Notes and references

1 H. Li, J. Wu, Z. Yin and H. Zhang, *Acc. Chem. Res.*, 2014, **47**, 1067–1075.
2 Z. Cai, B. Liu, X. Zou and H.-M. Cheng, *Chem. Rev.*, 2018, **118**, 6091–6133.

3 Y. Chen, Z. Fan, Z. Zhang, W. Niu, C. Li, N. Yang, B. Chen and H. Zhang, *Chem. Rev.*, 2018, **118**, 6409–6455.
4 M. Chhowalla, H. S. Shin, G. Eda, L.-J. Li, K. P. Loh and H. Zhang, *Nat. Chem.*, 2013, **5**, 263–275.
5 X. Yu, M. S. Prévot, N. Guijarro and K. Sivula, *Nat. Commun.*, 2015, **6**, 7596.
6 O. Lopez-Sanchez, D. Lembke, M. Kayci, A. Radenovic and A. Kis, *Nat. Nanotechnol.*, 2013, **8**, 497–501.
7 A. Castellanos-Gomez, *Nat. Photonics*, 2016, **10**, 202–204.
8 M. Buscema, J. O. Island, D. J. Groenendijk, S. I. Blanter, G. A. Steele, H. S. J. van der Zant and A. Castellanos-Gomez, *Chem. Soc. Rev.*, 2015, **44**, 3691–3718.
9 S. Tongay, J. Zhou, C. Ataca, J. Liu, J. S. Kang, T. S. Matthews, L. You, J. Li, J. C. Grossman and J. Wu, *Nano Lett.*, 2013, **13**, 2831–2836.
10 B. Radisavljevic, A. Radenovic, J. Brivio, V. Giacometti and A. Kis, *Nat. Nanotechnol.*, 2011, **6**, 147–150.
11 K. F. Mak and J. Shan, *Nat. Photonics*, 2016, **10**, 216–226.
12 A. Splendiani, L. Sun, Y. Zhang, T. Li, J. Kim, C. Y. Chim, G. Galli and F. Wang, *Nano Lett.*, 2010, **10**, 1271–1275.
13 Y. Zhang, T.-R. Chang, B. Zhou, Y.-T. Cui, H. Yan, Z. Liu, F. Schmitt, J. Lee, R. Moore, Y. Chen, H. Lin, H.-T. Jeng, S.-K. Mo, Z. Hussain, A. Bansil and Z.-X. Shen, *Nat. Nanotechnol.*, 2014, **9**, 111–115.
14 F. Xia, H. Wang, D. Xiao, M. Dubey and A. Ramasubramaniam, *Nat. Photonics*, 2014, **8**, 899–907.
15 A. F. Morpurgo, *Nat. Phys.*, 2013, **9**, 532–533.
16 Z. Ye, D. Sun and T. F. Heinz, *Nat. Phys.*, 2017, **13**, 26–29.
17 K. He, N. Kumar, L. Zhao, Z. Wang, K. F. Mak, H. Zhao and J. Shan, *Phys. Rev. Lett.*, 2014, **113**, 026803.
18 T.-Y. Wang, J.-L. Meng, Z.-Y. He, L. Chen, H. Zhu, Q.-Q. Sun, S.-J. Ding, P. Zhou and D. W. Zhang, *Adv. Sci.*, 2020, **7**, 1903480.
19 Q. Wang, N. Li, J. Tang, J. Zhu, Q. Zhang, Q. Jia, Y. Lu, Z. Wei, H. Yu, Y. Zhao, Y. Guo, L. Gu, G. Sun, W. Yang, R. Yang, D. Shi and G. Zhang, *Nano Lett.*, 2020, **20**, 7193–7199.
20 J. Du, H. Yu, B. Liu, M. Hong, Q. Liao, Z. Zhang and Y. Zhang, *Small Methods*, 2021, **5**, 2000919.
21 S. Cui, Z. Wen, X. Huang, J. Chang and J. Chen, *Small*, 2015, **11**, 2305–2313.
22 N. Rohaizad, C. C. Mayorga-Martinez, M. Fojtů, N. M. Latiff and M. Pumera, *Chem. Soc. Rev.*, 2021, **50**, 619–657.
23 D. S. Um, Y. Lee, S. Lim, S. Park, H. Lee and H. Ko, *ACS Appl. Mater. Interfaces*, 2016, **8**, 33955–33962.
24 J. S. Ross, P. Klement, A. M. Jones, N. J. Ghimire, J. Yan, D. G. Mandrus, T. Taniguchi, K. Watanabe, K. Kitamura, W. Yao, D. H. Cobden and X. Xu, *Nat. Nanotechnol.*, 2014, **9**, 268–272.
25 K. Wang, K. De Greve, L. A. Jauregui, A. Sushko, A. High, Y. Zhou, G. Scuri, T. Taniguchi, K. Watanabe, M. D. Lukin, H. Park and P. Kim, *Nat. Nanotechnol.*, 2018, **13**, 128–132.
26 M. L. Geier, T. J. Marks, L. J. Lauhon and M. C. Hersam, *Proc. Natl. Acad. Sci. U. S. A.*, 2013, **110**, 18076–18080.
27 J. S. Ross, S. Wu, H. Yu, N. J. Ghimire, A. M. Jones, G. Aivazian, J. Yan, D. G. Mandrus, D. Xiao, W. Yao and X. Xu, *Nat. Commun.*, 2013, **4**, 1474.
28 K. W. Lau, Calvin, Z. Gong, H. Yu and W. Yao, *Phys. Rev. B: Condens. Matter Mater. Phys.*, 2018, **98**, 115427.
29 S. Kasture, F. Lenzini, B. Haylock, A. Boes, A. Mitchell, E. W. Streed and M. Lobino, *J. Opt.*, 2016, **18**, 104007.
30 A. Boes, B. Corcoran, L. Chang, J. Bowers and A. Mitchell, *Laser Photonics Rev.*, 2018, **12**, 1700256.
31 H. Emami, N. Sarkhosh, L. A. Bui and A. Mitchell, *Opt. Express*, 2008, **16**, 13707–13712.
32 B. Wen, Y. Zhu, D. Yudistira, A. Boes, L. Zhang, T. Yidirim, B. Liu, H. Yan, X. Sun, Y. Zhou, Y. Xue, Y. Zhang, L. Fu, A. Mitchell, H. Zhang and Y. Lu, *ACS Nano*, 2019, **13**, 5335–5343.
33 L. Arizmendi and F. J. López-Barberá, *Appl. Phys. B*, 2006, **86**, 105.
34 K. Buse, A. Adibi and D. Psaltis, *Nature*, 1998, **393**, 665–668.
35 J. Baquedano, M. Carrascosa, L. Arizmendi and J. M. Cabrera, *J. Opt. Soc. Am. B*, 1987, **4**, 309–312.
36 D. L. Staebler, W. J. Burke, W. Phillips and J. J. Amodei, *Appl. Phys. Lett.*, 1975, **26**, 182–184.
37 D. L. Staebler and J. J. Amodei, *Ferroelectrics*, 1972, **3**, 107–113.
38 H. K. Shin, S. G. Lee and M. K. Lee, *Mater. Sci. Forum*, 2004, **449-452**, 981–984.
39 S. Zhang, H. M. Hill, K. Moudgil, C. A. Richter, A. R. Hight Walker, S. Barlow, S. R. Marder, C. A. Hacker and S. J. Pookpanratana, *Adv. Mater.*, 2018, **30**, 1802991.
40 S. Mouri, Y. Miyauchi and K. Matsuda, *Nano Lett.*, 2013, **13**, 5944–5948.
41 J. R. Schwesyg, H. A. Eggert, K. Buse, E. Śliwińska, S. Khalil, M. Kaiser and K. Meerholz, *Appl. Phys. B*, 2007, **89**, 15–17.
42 R. S. Weis and T. K. Gaylord, *Appl. Phys. A: Mater. Sci. Process.*, 1985, **37**, 191–203.
43 K. F. Mak, K. He, C. Lee, G. H. Lee, J. Hone, T. F. Heinz and J. Shan, *Nat. Mater.*, 2013, **12**, 207–211.
44 X. Zhang, H. Nan, S. Xiao, X. Wan, Z. Ni, X. Gu and K. Ostrikov, *ACS Appl. Mater. Interfaces*, 2017, **9**, 42121–42130.
45 K. P. Dhakal, D. L. Duong, J. Lee, H. Nam, M. Kim, M. Kan, Y. H. Lee and J. Kim, *Nanoscale*, 2014, **6**, 13028–13035.
46 J. Gorecki, V. Apostolopoulos, J.-Y. Ou, S. Mailis and N. Papasimakis, *ACS Nano*, 2018, **12**, 5940–5945.
47 A. Krumins, Z. Chen and T. Shiosaki, *Opt. Commun.*, 1995, **117**, 147–150.
48 L. Lucchetti, K. Kushnir, V. Reshetnyak, F. Ciciulla, A. Zaltron, C. Sada and F. Simoni, *Opt. Mater.*, 2017, **73**, 64–69.
49 T. H. Ly, Q. Deng, M. H. Doan, L.-J. Li and J. Zhao, *ACS Appl. Mater. Interfaces*, 2018, **10**, 29893–29901.

